

PAPER • OPEN ACCESS

## Study on Structural Characters of Nano-sized Hydroxyapatite Prepared from Limestone

To cite this article: Yuanita Amalia Hariyanto *et al* 2019 *IOP Conf. Ser.: Mater. Sci. Eng.* **515** 012020

View the [article online](#) for updates and enhancements.

# Study on Structural Characters of Nano-sized Hydroxyapatite Prepared from Limestone

Yuanita Amalia Hariyanto<sup>1</sup>, Ahmad Taufiq<sup>1,\*</sup>, Sunaryono<sup>1</sup>, Nandang Mufti<sup>1</sup>,  
Siriwat Soontaranon<sup>2</sup>, Nuntaporn Kamonsutthipaijit<sup>2</sup>

<sup>1</sup> Department of Physics, Faculty of Mathematics and Sciences, Universitas Negeri Malang (UM), Jl. Semarang 5, Malang 65145, Indonesia.

<sup>2</sup> Synchrotron Light Research Institute, Muang, Nakhon Ratchasima 30000, Thailand

\*Corresponding author's email: [ahmad.taufiq.fmipa@um.ac.id](mailto:ahmad.taufiq.fmipa@um.ac.id)

**Abstract.** In recent years, hydroxyapatite nanoparticles have exhibited excellent characters especially related to biomedical applications. Therefore, it is important to conduct the synthesis route development in simple and inexpensive ways. This work aimed to study the structural and optical characters of the hydroxyapatite nanoparticles prepared by precipitation route from natural limestone. The characterization results presented that the sample formed a pure hydroxyapatite with the hexagonal structure and sized in nanometric scale with the respective primary and secondary particles of 5 nm and 29 nm. The vibrational investigation exhibited that the prepared sample had functional groups of the hydroxyapatite originating from phosphate, carbonate, and hydroxyl. Furthermore, the hydroxyapatite had an optical bandgap of 3.38 eV.

**Keyword:** Hydroxyapatite, structure, nano-sized, hydroxyapatite, limestone.

## 1. Introduction

The recent studies related to material applications in the medical field has rapidly developed. Such enhancement is related to not only the technological aspect, but also the development of the new material for drug delivery systems. This is important since the developed material should be able to reach the target properly without causing the side effect in the healthy body tissue [1]. The requirement of the material that will be applied to drug delivery systems is the drug carrier should be able to release the medicine stably and properly [2]. On another side, the special study related to the nanostructure hierarchy is one of the initial requirements that should be done and fulfilled in the material fabrication before applying it.

From any kinds of the developed drug delivery systems, the nanosized-hydroxyapatite is frequent one developed in some medical applications since it has an excellent characteristic as the biomaterial including the performance of biocompatibility, bioactivity, bioresorbable, and osteoconductivity [3–5]. Moreover, hydroxyapatite nanoparticles have been also widely developed as the material of the substitute of bone, bone implant, and scaffolds composite for the tissue technique and gen delivery agent [1,6,7]. However, the hierarchy study of the nanostructure and optical characteristic of hydroxyapatite nanoparticles has not been deeply studied so far.



Besides the aspect of good nanostructure hierarchy, the preparation using simple and low-cost method is also important to study. Previous work showed that hydroxyapatite nanoparticles were prepared using microwave-assisted hydrothermal route [8]. This route has some excellences such as the easy and short-time fabrication process. However, the sizes of the obtained particles were in the range of 0.5-2  $\mu\text{m}$ . The other research used sol-gel method resulted in hydroxyapatite with the high purity and crystallinity but it used synthetic material and produced the size of particles ranging of 26 – 35 nm [9]. Another work also reported that synthesis of the hydroxyapatite with the basic material of limestone through solid state method was successfully conducted but the resulted crystallinity is still low and the produced size is in the collection of 26.85 – 40.84 nm [10]. In this research, the hydroxyapatite fabrication was conducted through precipitation method using natural limestone from Malang, Indonesia. The benefits of the method are such as the relatively short time, simple process, and low temperature.

## 2. Methods

The materials used were natural limestone taken from Malang, East Java – Indonesia,  $\text{NH}_4\text{OH}$ ,  $\text{HNO}_3$ ,  $(\text{NH}_4)_2\text{HPO}_4$ , and  $\text{H}_2\text{O}$ . The tools used were a magnetic stirrer, measuring cylinder, filter paper, pipette, crucible, mortar, beaker glass, and spatula. The fabrication of hydroxyapatite nanoparticles was carried out through precipitation method at the temperature of 70  $^\circ\text{C}$ . The calcium hydroxide was obtained from the calcination process for five hours and precipitated for some hours, reacted with  $\text{HNO}_3$  2M and stirred for 30 minutes. The titration of  $(\text{NH}_4)_2\text{HPO}_4$  for 60 minutes and the titration of  $\text{NH}_4\text{OH}$  to maintain pH. After that, the deposit was washed, filtered several times and dried. Hydroxyapatite nanoparticles were characterized using XRD to investigate the crystal structure. SAXS characterization was undertaken to study the distribution of particles of hydroxyapatite. Subsequently, to study the functional group of hydroxyapatite the characterization using FTIR spectrometer was done. Finally, UV-Vis characterization was completed to calculate the optical characteristic of the hydroxyapatite.

## 3. Results and Discussion

The diffractogram results of the diffraction pattern of hydroxyapatite are presented in Figure 1. Visually, the formed diffraction pattern indicates the form of hydroxyapatite sample. This case can be justified by the formed peaks at  $2\text{-theta} = 25.9^\circ, 31.9^\circ, 39.57^\circ, 46.62^\circ, 49.47^\circ$  [11]. The qualitative analysis showed that the formed diffraction pattern has a hexagonal construction (space group of  $P63/m$ ). That diffraction pattern has the same model with the standard pattern of AMCSD 0002281. This case implicated that the formed hydroxyapatite has the single phase without impurity. The hexagonal structure has the lattice parameter of  $a = b \neq c$  and  $V = (a^2c/2)\sqrt{3}$ . The results of the quantitative analysis showed that the hydroxyapatite sample has a hexagonal construction with the lattice constant of  $a = b = 9.448 \text{ \AA}$  and  $c = 6.861 \text{ \AA}$ . The mean of crystal size was analyzed with Scherrer's equation using the value of FWHM (full width at half maximum). The analysis yielded the crystallite size of 8.9 nm.

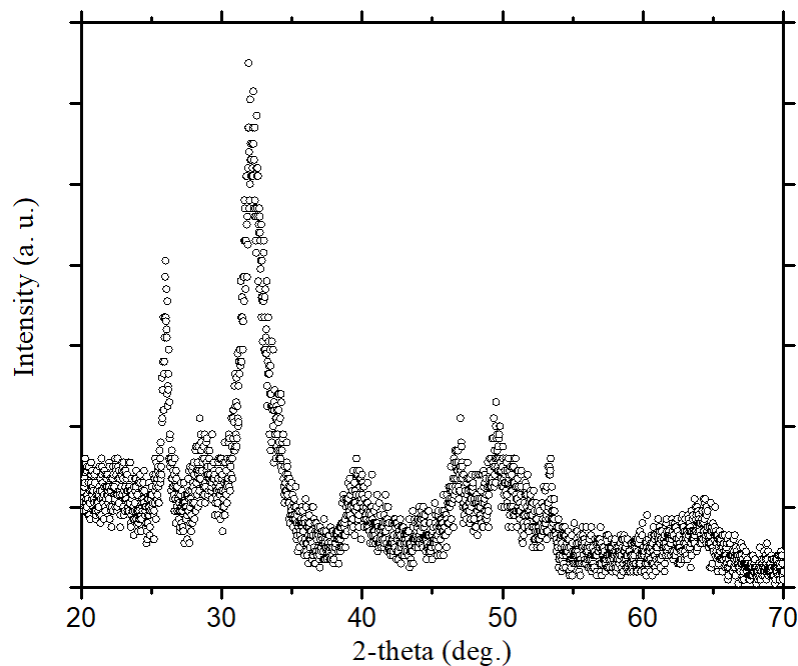


**Figure 1.** XRD patterns of Hydroxyapatite

On another side, the composition and distribution of hydroxyapatite ion could be analyzed for a 3-dimension structure as presented in Figure 2. In that crystal system, the number of ion of each cell unit was 44 ions distributed at 2 sites of Ca [Ca(1) dan Ca(2)], 1 site of P, 4 sites of oxygen [O(1), O(2), O(3), and O(4)], and 1 site of H along the  $c$  axis. Furthermore, the Ca(2) atom formed triangles at  $z = \frac{1}{4}$  and  $\frac{3}{4}$  at  $c$  axis, where O(4) and H atoms formed OH group oriented along the  $c$  axis and passing the center of Ca(2) triangle. Meanwhile, the P atom formed PO<sub>4</sub> [O(1), O(2), and 2 O(3)] groups with tetrahedral structure. Finally, the PO<sub>4</sub> group was connected along  $c$  axis by Ca(1) and Ca(2) atoms [12].

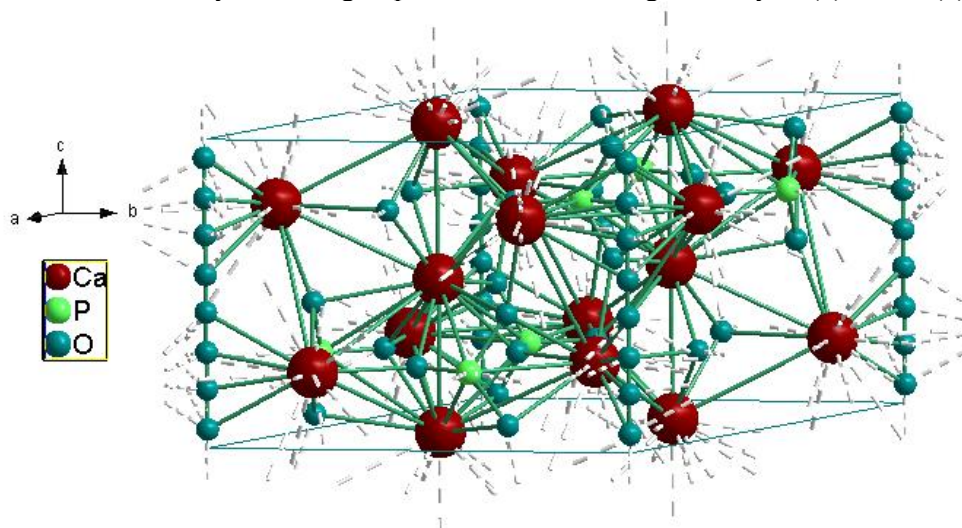


**Figure 2.** Three-dimensional structure of hydroxyapatite

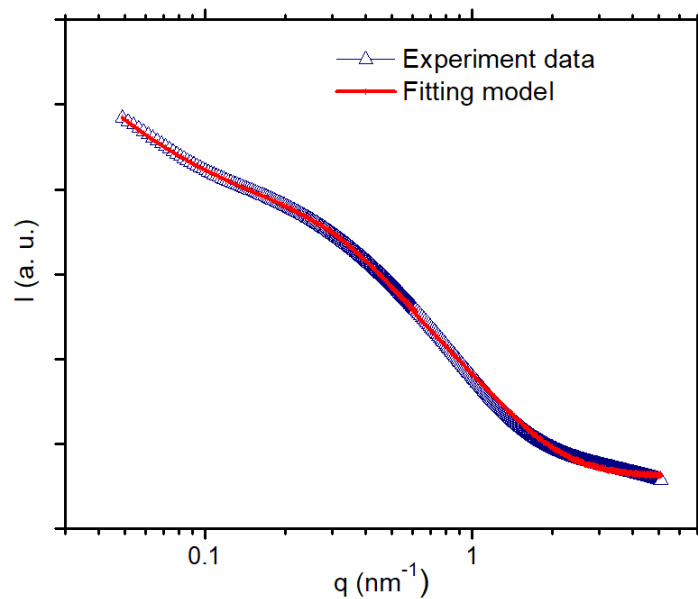


**Figure 3.** SAXS curve of hydroxyapatite nanoparticles

SAXS curve of hydroxyapatite samples was shown in Figure 3. Visually, the fitting results appeared on all ranges of  $q$  in accordance with the calculation of the theoretical model. The curve at the range of high  $q$  represents the smallest particle size called primary particle. At the range of low  $q$ , the gradient of the curve represents the mass fractal. Physically, this case shows that the primary particles experience the aggregation/agglomeration to form the fractal mass structure. The quantitative analysis of hydroxyapatite sample was fitted using 2 lognormal spherical model as the form factor to know the distribution of the size of primary and secondary particles. The structural factor ( $S$ ) of hydroxyapatite sample was fitted using a mass fractal model as presented in Equation 1 [13].

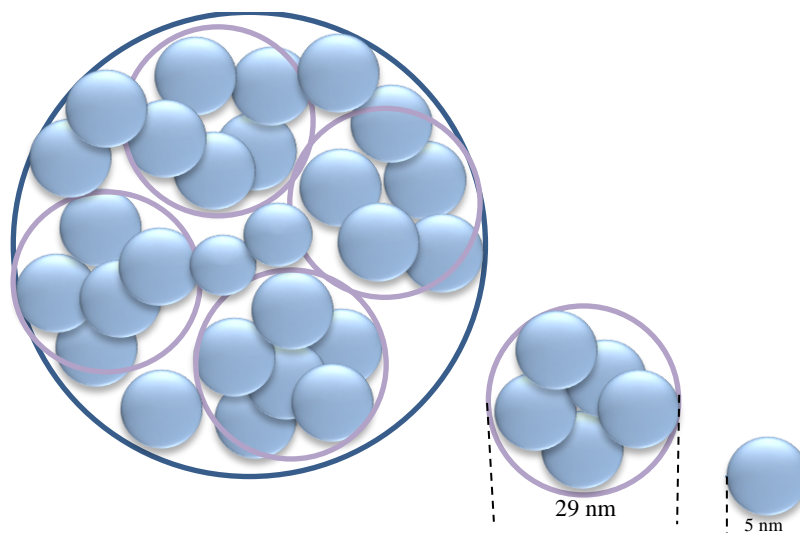


**Figure 4.** The hierarchical structure of hydroxyapatite

$$S_{\text{exp}}(q, \xi, D, R) = 1 + \frac{D\Gamma(D-1)\sin([D-1]\tan^{-1}(q\xi))}{(qR)^D \left[1 + \frac{1}{q^2\xi^2}\right]^{(D-1)/2}} \quad (1)$$

where  $D$  is a fractal dimension,  $\Gamma$  is gamma function,  $q$  is a scattering vector, and  $\xi$  is cutoff space.

The fitting results showed that the hydroxyapatite sample has the primary particle with 55 nm size and the secondary particles with 29.6 nm size. Such particles agglomerated to form a cluster. The cluster formation was influenced by the interaction between nanoparticles. The visualization of the hierarchical structure of the sample can be found in Figure 4. Based on the fitting results using the mass fractal approach, the  $D$  value was 3.2. Such value showed that the sample had the massive structure in 3-dimension. Such value also implicated that the hydroxyapatite had a smooth surface [14].

Based on the data presented in Figure 5, the results of FTIR characterization showed almost similar results compared to the previous research. This case was shown by the atomic vibration at a certain wavenumber. The vibrations of the formed functional group were such as phosphate, carbonate, and hydroxyl functional groups (Table 1). The vibrations of the phosphate functional group occurred at the four wavenumbers were such as 576, 608, 964, and 1041  $\text{cm}^{-1}$ . The vibrations of the carbonate functional group happened at the band of 878, 1419, and 1636  $\text{cm}^{-1}$ . These research results were in line with the report of previous works presenting that the vibration of carbonate functional group at the wavelength of 877  $\text{cm}^{-1}$  and 1300 – 1650  $\text{cm}^{-1}$  [15,16]. Furthermore, at the wavenumber of 3372  $\text{cm}^{-1}$ , the vibration of O-H stretching occurred.

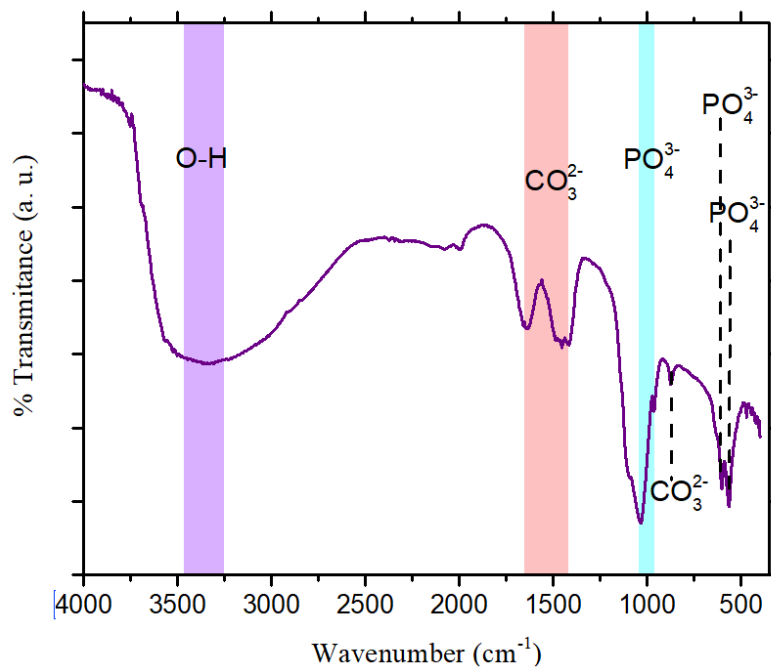


**Figure 5.** The functional groups of hydroxyapatite

**Table 1.** The functional group of the synthesized hydroxyapatite

| Wavenumber (cm <sup>-1</sup> ) | Functional groups | References |
|--------------------------------|-------------------|------------|
| 576, 608, 964, 1041            | $PO_4^{3-}$       | [15]       |
| 878, 1419, 1636                | $CO_3^{2-}$       | [15,16]    |
| 3372                           | $O-H$             | [17]       |

The value of hydroxyapatite gap energy could be obtained from the linear fitting using the Kubelka-Munk equation by doing the graphics plot of the relationship between  $(\alpha h\nu)^2$  and  $h\nu$ . The Kubelka-Munk equation is written in Equation 2 [16].

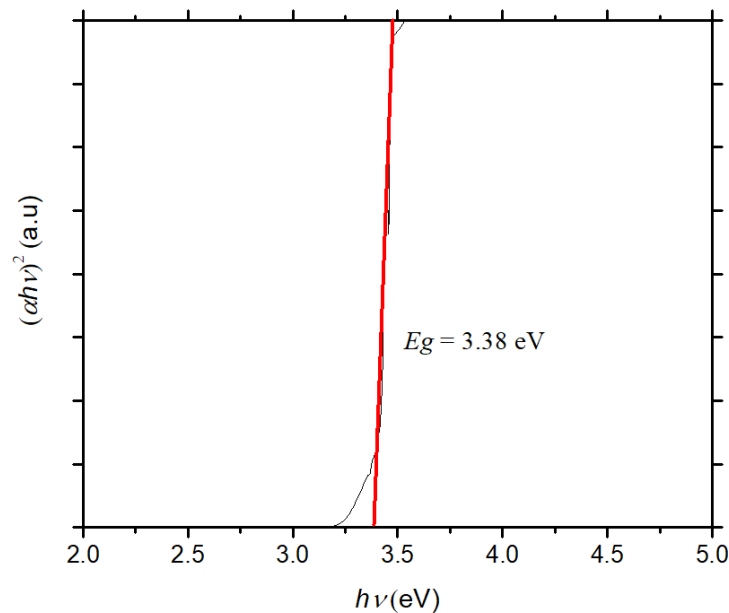
$$\alpha h\nu = B(h\nu - E_g)^n \quad (2)$$

$h\nu$  = Photon energy

$B$  = Constant

$E_g$  = bandgap energy

$n$  = Constant for indirect gap (2)

**Figure 6.** Bandgap value of hydroxyapatite

The linear fitting resulted in the gap energy value of hydroxyapatite sample of 3.38 eV using the calculation of indirect gap [16]. Such value was at the range of the research conducted by Aronov *et al.* reporting that some values of gap energy in every situation of hydroxyapatite were at the range of 2.6 eV – 3.9 eV [18]. Such values indicated that when the hydroxyapatite was irradiated by UV, the UV irradiation caused the oxygen vacancy at the lattice of hydroxyapatite. Such thing caused the electron in the valence band moved and bound by the oxygen in the atmosphere creating the free radical oxygen. This case implicated that the hydroxyapatite has good potential if it is applied for photocatalyst.

#### 4. Conclusion

The hydroxyapatite nanoparticles formed the hexagonal construction with the lattice constant of  $a = b = 9.448 \text{ \AA}$  and  $c = 6.861 \text{ \AA}$ . The size of primary particles was 5 nm and they underwent aggregation to form the secondary particles of 29.6 nm. The hydroxyapatite nanoparticles formed a cluster with the massive structure of 3-dimension. The optical characteristic of hydroxyapatite nanoparticles had the bandgap of 3.38 eV. Thereby, the prepared hydroxyapatite nanoparticles in this work have a big potential for further application.

#### References

- [1] Gu L, He X and Wu Z 2014 Mesoporous Fe<sub>3</sub>O<sub>4</sub>/hydroxyapatite composite for targeted drug delivery Mater. Res. Bull. **59** 65–68
- [2] Pundir S, Badola A and Sharma D 2017 Sustained release matrix technology and recent advance in matrix drug delivery system: a review Int. J. Drug Res. Technol. **3** 8
- [3] Luo Y, Ling Y, Guo W, Pang J, Liu W, Fang Y, Wen X, Wei K and Gao X 2010 Docetaxel loaded oleic acid-coated hydroxyapatite nanoparticles enhance the docetaxel-induced apoptosis through activation of caspase-2 in androgen independent prostate cancer cells J. Controlled Release **147** 278–88
- [4] Venkatasubbu G D, Ramasamy S, Avadhani G S, Ramakrishnan V and Kumar J 2013 Surface modification and paclitaxel drug delivery of folic acid modified polyethylene glycol functionalized hydroxyapatite nanoparticles Powder Technol. **235** 437–442
- [5] Ylinen P 2006 Applications of coralline hydroxyapatite with bioabsorbable containment and reinforcement as bone graft substitute: An experimental study
- [6] Joschek S, Nies B, Krotz R and Göpferich A 2000 Chemical and physicochemical characterization of porous hydroxyapatite ceramics made of natural bone Biomaterials **21** 1645–58
- [7] Jiménez Flores Y, Suárez-Quezada M, Rojas-Trigos J, Lartundo-Rojas L, Suárez V and Mantilla A 2017 Characterization of Tb-doped hydroxyapatite for biomedical applications: optical properties and energy band gap determination J. Mater. Sci. **52** 1–11
- [8] Wang K-W, Zhu Y-J, Chen F, Cheng G-F and Huang Y-H 2011 Microwave-assisted synthesis of hydroxyapatite hollow microspheres in aqueous solution Mater. Lett. **65** 2361–2363
- [9] Kaygili O, Dorozhkin S V and Keser S 2014 Synthesis and characterization of Ce-substituted hydroxyapatite by sol–gel method Mater. Sci. Eng. C **42** 78–82
- [10] Hartatiek, Yudyanto, Ratnasari S D, Windari R Y and Hidayat N 2017 Solid State Reaction Synthesis of Si-HA as Potential Biomedical Material: An Endeavor to Enhance the Added Value of Indonesian Mineral Resources IOP Conf. Ser. Mater. Sci. Eng. **202** 012021
- [11] Dong L, Zhu Z, Qiu Y and Zhao J 2010 Removal of lead from aqueous solution by hydroxyapatite/magnetite composite adsorbent Chem. Eng. J. **165** 827–34
- [12] Matsunaga K and Kuwabara A 2007 First-principles study of vacancy formation in hydroxyapatite Phys. Rev. B **75** 014102
- [13] Taufiq A, Putra E G R, Okazawa A, Watanabe I, Kojima N and Pratapa S 2015 Nanoscale Clustering and Magnetic Properties of Mn<sub>x</sub>Fe<sub>3-x</sub>O<sub>4</sub> Particles Prepared from Natural Magnetite J. Supercond. Nov. Magn. **28** 2855–2863



- [14] Gelli R, Del Buffa S, Tempesti P, Bonini M, Ridi F and Baglioni P 2018 Enhanced formation of hydroxyapatites in gelatin/imogolite macroporous hydrogels *J. Colloid Interface Sci.* **511** 145–154
- [15] Rehman I and Bonfield W 1997 Characterization of hydroxyapatite and carbonated apatite by photo acoustic FTIR spectroscopy *J. Mater. Sci. Mater. Med.* **8** 1–4
- [16] Valizadeh S, Rasoulifard M H and Dorraji M S 2014 Modified Fe<sub>3</sub>O<sub>4</sub>-hydroxyapatite nanocomposites as heterogeneous catalysts in three UV, Vis and Fenton like degradation systems *Appl. Surf. Sci.* **319** 358–366
- [17] Zayed M A, Ahmed M A, Imam N G and El Sherbiny D H 2016 Preparation and structure characterization of hematite/magnetite ferro-fluid nanocomposites for hyperthermia purposes *J. Mol. Liq.* **222** 895–905
- [18] Aronov D, Karlov A and Rosenman G 2007 Hydroxyapatite nanoceramics: Basic physical properties and biointerface modification *J. Eur. Ceram. Soc.* **27** 4181–4186

### Acknowledgments

This work was supported by PNBPN Universitas Negeri Malang for AT in 2018.